URN (Paper): urn:nbn:de:gbv:ilm1-2011iwk-094:3

56TH INTERNATIONAL SCIENTIFIC COLLOQUIUM

Ilmenau University of Technology, 12 – 16 September 2011
URN: urn:nbn:gbv:ilm1-2011iwk:5

SPECTROSCOPIC DETERMINATION OF THE EFFECTIVE HUMIDITY FOR DISTANCE MEASUREMENTS IN AIR

Florian Pollinger, Karl Meiners-Hagen, Nicolae R. Doloca, and Ahmed Abou-Zeid

Physikalisch-Technische Bundesanstalt, Bundesallee 100, 38116 Braunschweig

ABSTRACT

In geodetic and in industrial applications, length measurements are performed over longer distances in uncontrolled environments. Relative measurement uncertainties in the order of 10^{-7} in an optical length can only be achieved if the index of refraction can be determined with the same level of uncertainty. One parameter for the application of respective approximation formulas is the humidity of the traversed air. To determine the effective humidity along the whole path of the length probe, an optical technique was realized in this study based on quantitative absorption spectroscopy. The spectrometer was designed to be combined with optical distance meters. Comparisons to conventional sensors under well-controlled environmental conditions proof the capability of the concept with an agreement significantly better than 4 % relative humidity (*RH*), the level necessary to achieve measurement uncertainties of 10^{-7} of the length measurement in a wider temperature range. The advantages of the optical approach, sensitivity to the effective humidity and fast response times, are demonstrated in uncontrolled conditions.

Index Terms **–** tunable diode laser absorption spectroscopy, humidity, air refractive index, length metrology, long distance

1. INTRODUCTION

Interferometric length measurements in vacuum conditions achieve lower and lower levels of uncertainty, providing sub-nanometer resolutions (e.g. [1]). But it is not only the methodology advancing, the practical need for high-accuracy measurement increases constantly. Not at least, measurements of longer distances above one meter up to several hundred meters have raised increased attention in the last years [2 - 5], driven both, by the manufacturing sector, e.g. in aerospace industries, and by special applications in astronomy or geodesy , like the surveillance of nuclear waste repositories, for which relative measurement uncertainties better than 10^{-6} are required. When applied for these longer distances in the real world, however, one has to deal with non-cooperative environments. Optimum conditions, like vacuum or at least air-conditioning are practically not possible.

Therefore, the interferometric length measurement is only one part of the challenge to measure long distances in air. As the scale of such a traceable measurement is ultimately the speed of light in the environment, the index of refraction n must be determined. Indeed, for state of the art geodetic distance meters, the relative uncertainty of the total measurement is dominated by the uncertainty of the knowledge of the index of refraction. It is conventionally determined using empirical equations [6 – 8] with temperature, humidity, pressure, and CO_2 concentration as parameters. Amongst those, the effective temperature along the beam is the most difficult and most critical of these parameters to be determined for longer distances. Outdoors, or even in factory halls, local sources of heat and humidity, like machines, cars or trees, e.g., induce in part fast changes, but also lead to stronger local variations in temperature. The impact on the interpretation of the result of the length measurement of such variations, on the other hand, is highly significant: A difference of 1 K corresponds to a relative change in air refractivity of 1×10^{-6}, limiting the uncertainty of the complete length measurement to the same level. As a consequence, a number of techniques have been developed to determine the effective temperature along a beam, using, e.g., acoustic density [9], or the population ratio of vibrational levels [10 - 12].

The most viable approach, however, is the interferometric measurement of the length using both the fundamental and the second harmonic wavelength of a laser source. Deploying the knowledge on the functional dependence of the dispersion, the influence of the index of refraction can be cancelled out [13 – 15] For the application in wet, i.e. “real air”, however, the humidity in the beam must be known better than 4% in order to get uncertainties below $10^{-7}l$ with this method [16]. Given the targeted long distances and the local fast variations within the beam track, even such a relatively moderate demand poses a serious challenge for the sensor system. These challenges are optimally matched by an optical probe: (1) the beam traverses the same measurement volume as the length probe and (2) the response time is only limited by the sweep frequency over the absorptive feature. Optical humidity sensors based on tunable diode laser absorption spectroscopy (TDLAS) have been reported for over two decades (e.g. [17 - 21] and references therein). But these techniques were mainly developed for well-defined absorption volumes used in high precision spectroscopy, like Herriot cells. We present two realizations of an optical hygrometer which were designed for free path long distance measurements. One of these hygrometers was successfully combined with a four-wavelength interferometer [22] to form a complete refractivity-compensated distance meter.

2. THEORY

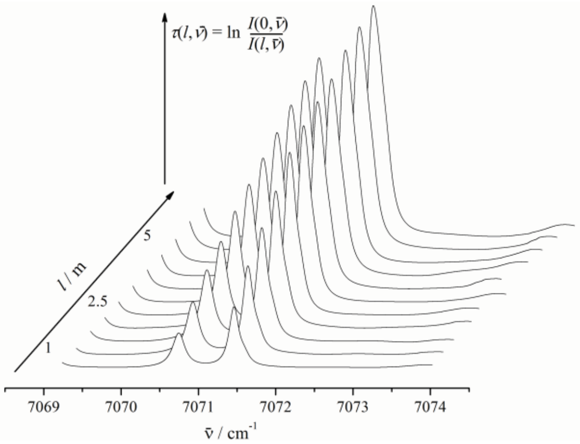

Figure 1. Length dependence of the absorption signal. The evolution of the strongest absorption feature in fig. 3 is depicted.

The measurement principle of most optical hygrometers is based on the classical Beer-Lambert law of absorption

$$I(l) = I_0 e^{-\tau(l)} \tag{1}$$

relating the transmitted intensity $I(l)$ to the primary intensity I_0 with the help of the dimensionless optical depth $\tau(l)$. As exemplified in fig. 1, the optical depth is in principal directly proportional to the absorption path length l. In spectral regions in which molecular transitions of traversed molecules are located the optical density $\tau(l)$ is predominantly determined by absorption processes. In this case, it depends on parameters describing the molecular absorption processes and the number density u of the absorbing molecular species. The latter quantity is a direct measure of the humidity.

To extract the desired number density u, it is beneficial to deploy eq. (1) in a limited frequency interval $[\nu_1, \nu_2]$ [17]. The integral of equation (1) can be rearranged in a relatively simple form [23] using the notation of the renowned HITRAN database [24]:

$$\tau(l) = \int_{\nu_1}^{\nu_2} \ln\left(\frac{I_0}{I}\right) d\nu = ul \sum_j S_j(T) \Big|_{\nu_1}^{\nu_2} \tag{2}$$

As the line strength $S_j(T)$ at the deployed temperature T can be deduced from the updated HITRAN database [25], equation (2) can be used to determine the number density u of the water molecules in the beam path from the normalized absorption I/I_0. The number density u can then be converted into the more common quantities to describe the humidity, partial water pressure e or relative humidity RH, by deploying the ideal gas law and by well-established approximation formulae [26].

3. EXPERIMENTAL METHODS

Equation (2) provides a direct instruction for the experimental realization of a spectroscopy-based hygrometer. Two diode-laser based hygrometers were realized based on this principle in this study, in combination covering a range between several centimeters up several hundred meters.

3.1. Short range hygrometer

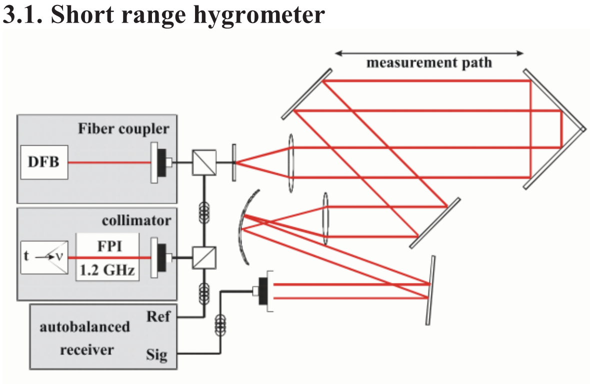

Figure 2. Set-up of the DFB-laser based short range hygrometer.

To realize an optical hygrometer based on eq. (2), a molecular transition must be sampled by a laser sweep over the complete absorption feature. For the quantitative analysis of the absorption, it is advantageous to work in an unsaturated absorption regime, with a transmission of 40 - 90 %. For transmissions of approximately 80 – 90 %, the tails of the absorption peaks are less pronounced and therefore, the identification of the background level is less problematic. The frequency window to be sampled can hence be kept smaller. If the transmission exceeds approximately 90 %, however, the contrast of the absorption lines gets too small, and the influence of noise increases significantly. Therefore, the choice of the absorption band and thus of a suitable absorption strength determines the accessible range of the optical hygrometer. For a range up to approximately ten meters, the absorption band of the water molecule in the telecom regime around 1400 nm provides suitable absorption strengths.

In fig. 2 a realization of a hygrometer for shorter distances is depicted. As light source, a DFB diode laser at 1405 nm with a mode-hop free spectral range (MHFSR) of several hundred GHz is deployed. The beam is split into reference and measuring beam. During the modulation, the frequency change is calibrated by a Fabry-Perot interferometer (FPI). It is based on a solid etalon to enhance stability and provides a free spectral range (FSR) of 1.2 GHz. The absolute value of the laser frequency can be determined by an optical spectrum analyzer (OSA) and in-situ by the absolute position of the transition as listed in the HITRAN database [25]. The measuring beam is expanded, displaced and reflected back by a 50.8 mm corner cube. The absorption signal is finally extracted by an autobalanced detector (New Focus 2017). All signals are collected by a 16-bit, 8 channel data acquisition card (National instruments). The recorded spectra are then normalized assuming a linear background and numerically integrated. Typically, ten spectra with a repetition rate of 10 Hz are sampled, averaged and then integrated.

In fig. 3, the spectral range accessible to the deployed DFB diode is depicted. Three spectral duplets are located within this range. According to the HITRAN database [25], the three duplets are formed by a multitude of transitions. Of the three duplets, the spectral feature around 7069 cm^{-1} is the least suitable for a quantitative analysis: it consists of a large number of transitions which moreover are distributed over a relatively wide frequency range between 7068 and 7069.3 cm^{-1}. Therefore, the identification of a baseline is difficult in this case. The other two duplets, however, are narrower, and thus more convenient for analysis. The absorption strength of both transition groups are different enough that ranges between several centimeters and approximately ten meters can be probed with this hygrometer.

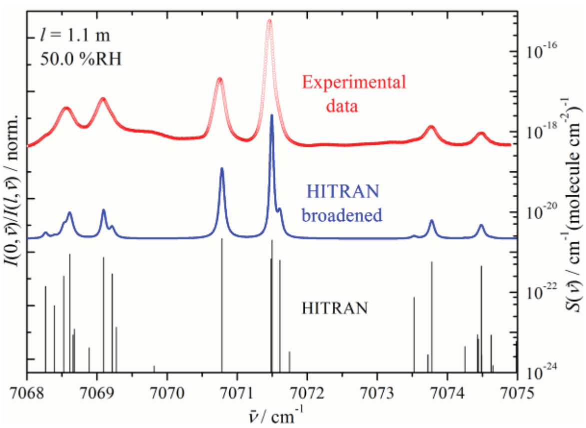

Figure 3. Absorption transitions within the spectral range of the DFB laser diode of the short range hygrometer. The line strengths S have been taken out of the HITRAN database [25].

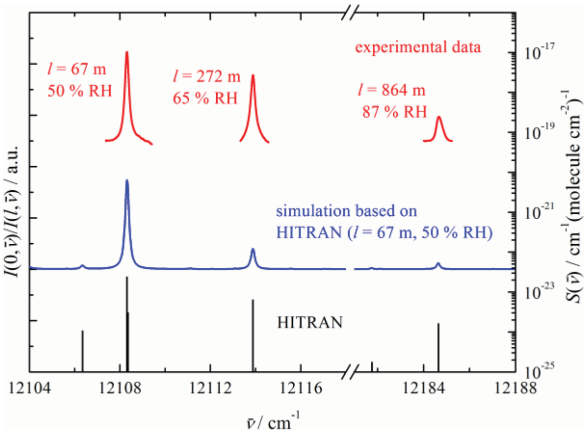

Figure 4. Absorption transitions deployed for the long range hygrometer. Experimental data was taken under different conditions. Line strengths have been taken out of the HITRAN database [25].

To deduce the humidity of the absorption data, complementary information on the ambient conditions is necessary. Ambient pressure p and temperature T were recorded using a commercial calibrated pressure sensor (Setra B370) and a network of at least two Pt-100 temperature sensors.

3.2. Long range hygrometer

For the application in geodetic length measurement, however, a distance range between a few meters up to one kilometer must be covered by an ideal hygrometer. Hence, the spectral working point of the spectrometer must be more flexible to cover the complete distance range. Therefore, a hygrometer based on an external cavity diode laser (ECDL, Toptica DLpro) was developed for flexible outdoor measurements. Using this source, the complete water absorption band between 800 and 850 nm is accessible. The line strengths of the respective transitions are about two orders of magnitude smaller then the line strengths in the telecom regime. In fig. 4, three isolated transitions within that band are depicted which are used in the long range hygrometer to determine the humidity over distances between twenty-five and several hundred meters. The HITRAN database, however, is for the weaker absorption lines

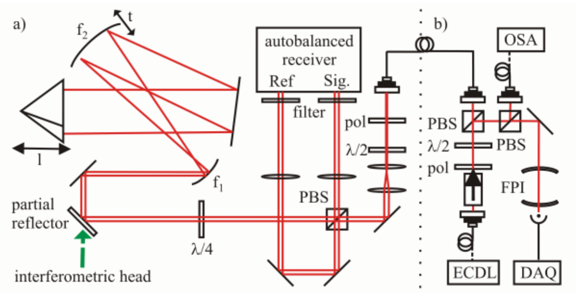

Figure 5. Set-up of the long range hygrometer. Spectroscopic head (a) and beam preparation unit (b) are separated.

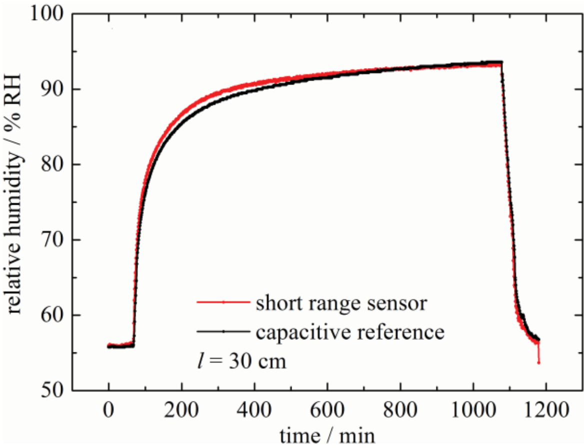

Figure 6. Performance of the short range sensor in a climate chamber. The optical hygrometer reacts slightly quicker to changes of the ambient conditions.

in this band less reliable then in the telecom band. In fact, the respective line strengths have to be calibrated when used for quantitative spectroscopy. Deviations from the literature values of over 10 % have been observed [23].

In detail, the spectrometer is divided into two functional units: the spectrometer head (fig. 5a) and the beam preparation unit (fig. 5b), connected by a polarization maintaining optical fiber. The modular functional design corresponds to the design of the short range hygrometer. For frequency-calibration a commercial temperature-controlled FPI with a FSR of 1.0 GHz is deployed (Toptica FPI 100). Probe and reference beam are only separated on the spectrometer head before the beam expansion. The expansion unit is set-up completely by achromatic reflective optics. Therefore, the hygrometer can be easily combined with a four wavelength interferometer [22]. Data acquisition and processing are performed in complete analogy to the short range hygrometer. A challenge for the analysis is the fact, however, that the MHFSR of the deployed ECDL does not exceed several tens of GHz, in particular when applied under difficult environmental conditions. As can be seen in fig. 4, typically only one absorption feature can be sampled by such a MHFSR. If the absorption feature can even only be partially resolved, a refined analysis based on partial integration and increased modeling effort is necessary [23].

4. EXPERIMENTAL RESULTS

Both hygrometers were characterized under well-controlled and under real life conditions. The results are in good agreement with the specified uncertainty goals for the compensation of length measurements.

4.1. Verification of performance

The performance of the optical hygrometers was verified both for varying environmental conditions and for different measurement lengths. In fig. 6 the sensitivity of the short range sensor to changing humidity is depicted. The short range hygrometer was placed into an improvised climate chamber together with a calibrated reference hygrometer (Testo 650). Due to the relatively short optical absorption path of 30 cm, the strongest absorption feature at 7071.5 cm^{-1} was analyzed. The data of reference and optical hygrometer was logged simultaneously every minute. A wet sponge was used to induce a humidity variation in the chamber. After approximately 67 minutes, it was introduced into the chamber, and after 1070 minutes taken out. Both signals agree well during the humidity step, deviations remaining safely below the 4 % limit. The largest deviations are observed in the dynamic behavior after introduction and extraction of the humidity source. The optical hygrometer reacts in both cases slightly quicker to the changing conditions.

Figure 7 shows the result of an experiment investigating the distance-dependence of the deviation between reference and optical hygrometer. The longer distances were investigated using the absorption features at 7074 cm^{-1}. The measurement was performed within the geodetic base of the Physikalisch-Technische Bundesanstalt (PTB), the national metrology institute of Germany. The room is air-conditioned, the humidity during the depicted experiment being kept at approximately 50 % RH. During the measurements, the room was vacated. The reference humidity sensor was placed close to the optical measurement path. The humidity was measured approximately every 50 cm. At each location, the measurement was performed for ten minutes, sampling ten sweeps every thirty seconds. The error bars given in fig. 7 indicate the standard deviation of these measurements. Up to approximately

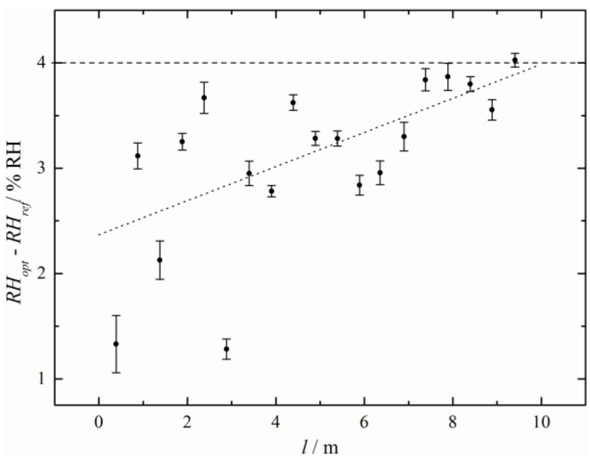

Figure 7. Length dependency of the short range hygrometer. Each data point represents a ten minute average of 20 measurements at the respective position. The error bars indicate the corresponding standard deviation. Up to approximately 10 m, optical and reference sensor agree within 4 % RH.

ten meters, optical and reference sensors agree within 4 % RH, the optical value being systematically larger than the reference one. The deviation increases with growing measurement distance as indicated by the dotted line in fig. 7. The analysis was performed using the line strength parameter of the HITRAN database. The offset of approximately 2 % relative humidity can be explained by the uncertainty of 3 % of the database and can be removed by a recalibration of the respective line strength. The systematic increase of deviation, however, can be associated with the spectral properties of the selected part of the absorption band. The spectral absorption features get broader with increased absorption. Thus, the identification of the background level gets more and more difficult with increasing absorption length. The tendency of the deviation can well be explained by an increasing contribution of the tails of the strong absorption feature at 7071.5 cm^{-1} to the detected absorption at 7074 cm^{-1}. This effect limits the range of the hygrometer in this configuration. For longer distances, more isolated and weaker lines are necessary.

The long range sensor was verified in laboratory at MIKES, the national metrology institute of Finland, in which the humidity can be actively controlled. It was compared against a network of four calibrated humidity sensors (Vaisala HMP45AL) and an optical hygrometer based on a slightly different approach [23]. The comparison against the conventional network depicted in fig. 8 shows an excellent agreement between reference and optical sensor, safely within the 4 % RH uncertainty band indicated by the arrow. The absorption strength S of the analyzed absorption duplet line at 12108.3 cm^{-1}, however, had to be recalibrated by 2.9 % before. Details on the experimental design and the analysis of the comparison can be found in reference [23].

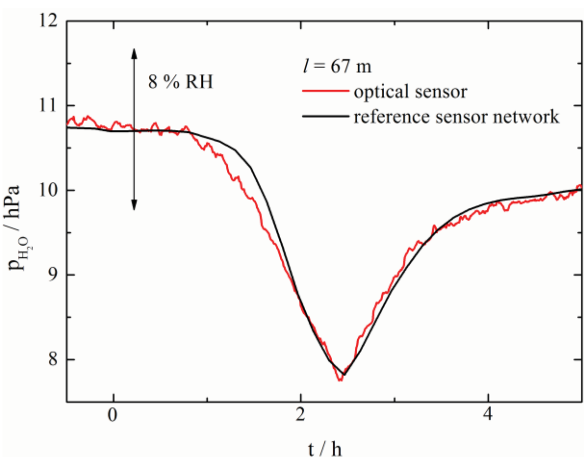

Figure 8. Comparison of the long range hygrometer against a network of calibrated capacitive sensors [23].

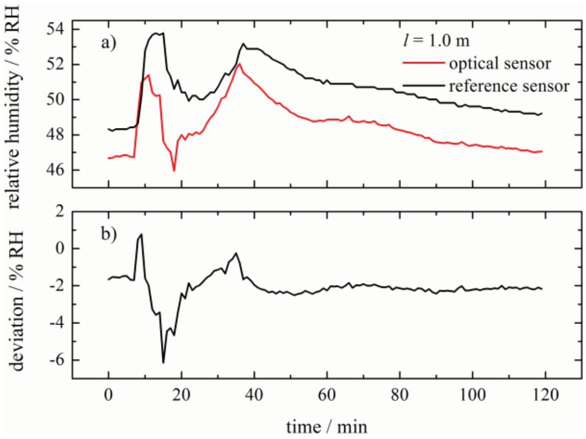

Figure 9. Performance of the short range hygrometer under uncontrolled conditions. a) Readings of the two sensor systems. b) Deviation of the optical from the capacitive sensor. The data was recorded during a laboratory visit of approximately 20 people.

4.2. Dynamic measurements

Based on the experience of the verification experiments, the hygrometers were also deployed under “uncontrolled environments”. Two examples are discussed in the following section.

One example for such a “dynamic measurement” is depicted in fig. 9. During a laboratory visit of approximately 20 people, i.e. point sources of humidity in this context, the readings of the short range hygrometer and the reference hygrometer (Testo 650) were recorded. An absorption path of 1 m was chosen and the reference sensor placed close to the probe beam. As can be seen in fig. 9b, both measurements agree within 4 % RH except of a single data point. The offset of 2 % RH is in agreement with the observation under controlled environment (fig. 7). In detail, there are however distinct differences in the response behavior of both sensors. For once, the optical sensor reacts again slightly quicker to changes, the amplitude of the humidity variations exceeding the response of the optical sensor by up to 0.5 % RH.

Similar observations can be made when investigating the performance of the long range sensor outdoors. In fig. 10 a measurement over 272 m on the geodetic baseline at Innsbruck (Austria) is depicted. The optical hygrometer was compared to a network of three calibrated humidity sensors. The depicted temperature was deduced from a network of seven Pt-100 sensors which were evenly distributed along the measurement path. The baseline is located close to a highway. Therefore, fast and frequent local variations both in temperature and in humidity have to be taken into account. Unfortunately, dust from the highway led to a continuous contamination of the optics, making a calibration on site necessary.

The functional dependence of optical and reference humidity readings are in reasonable agreement.

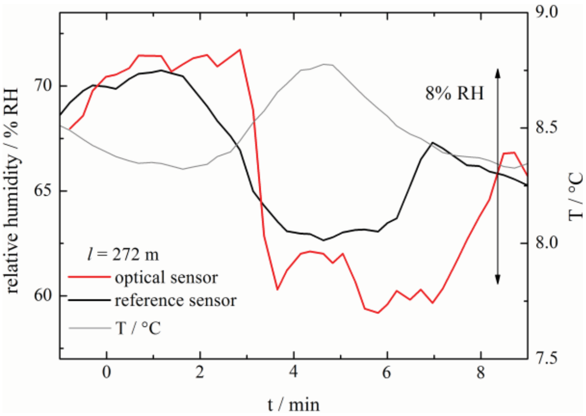

Figure 10. Performance of the optical sensor under uncontrolled environmental conditions. Optical sensor and reference network differ significantly [23].

Amplitudes and onsets differ significantly, although the overall agreement remains almost all the time within the 4 % uncertainty band [23]. The fast changes on minute scale are the result of the challenging environment. Details on this experiment and its analysis can be found in reference [23].

5. CONCLUSIONS

The design of a flexible optical hygrometer is a non-trivial task. In principle, for every combination of distance and humidity an optimum transition for the humidity determination must be identified. Therefore, the demands for the optical source are highly challenging. Furthermore, the quality of the quantitative analysis depends highly on the uncertainty of the literature parameters used in the analysis. In the case of weaker absorption lines, a calibration of the instruments gets almost inevitable. Nevertheless, the hygrometers presented in this study fulfill the requirements necessary to perform refractivity-compensated length measurements. Both sensors have proven their performance in benchmark experiments under well-controlled conditions. Based on these experiments, one can conclude that the deviations in the dynamic measurements from the “reference” are not a shortfall of the optical method, but proof the benefit of the large effort. The optical hygrometer is in fact sensitive to the effective humidity along the complete beam path, while a capacitive sensor only samples the immediate vicinity of the sensor head. If the environment is inhomogeneous and even fast changing, a correct measurement of the humidity would require a dense net of capacitive sensors. Although the deviations remain within the 4 % uncertainty margin for a refractivity compensation of the length measurement in the investigated cases, a fast high precision long distance measurement is obviously supported by an optical hygrometer, in particular in non-trivial environmental conditions.

ACKNOWLEDGMENTS

This research is in part funded by the European Community’s Seventh Framework Programme ERA-NET Plus, under grant agreement 217257. The research was performed within the EURAMET joint research project ‘Absolute Long-distance Measurement in Air’. The authors would like to thank T. Hieta, M. Merimaa and M. Vainio from MIKES, Finland for providing the simulation data of the 820 nm band, the preparation and host of the hygrometer comparisons, and for valuable discussions. The measurements at Innsbruck were supported by B. Steffan and H. Skorpil from BEV, Austria. Last but not least, the authors would like to acknowledge technical assistance by J. Beyer and K. Makhonina, and the influence of valuable experience gathered in earlier work by H. J. Altmeyer.

[1] R. Köning, J. Flügge, and H. Bosse, “Achievement of sub nanometer reproducibility in line scale measurements with the nanometer comparator”, Proc. SPIE 6518, 65183F (2007)

[2] J.-P. Wallerand et al., “Towards new absolute long distance measurement in air”, NCSL Int. Workshop and Symp. (Orlando, USA) (2008)

[3] I. Coddington, C. Swann, L. Nenadovic, and N. Newbury, “Rapid and precise absolute distance measurements at long range”, Nat. Photon. 3, 351-356 (2009)

[4] F. Pollinger, N. R. Doloca, K. Meiners-Hagen, M. Wedde, and A. Abou-Zeid, “Measurements of absolute long distances”, Proc. SPIE 7544, 754445 (2010)

[5] G. N. Peggs et al., “Recent developments in large-scale dimensional metrology, Proc. Inst. Mech. Eng. B: J. Eng. Man. 223, 571-595 (2009)

[6] B. Edlén, “The Refractive Index of Air”, Metrologia 2, 71-80 (1966)

[7] G. Bönsch and E. Potulski, “Measurement of the refractive index of air and comparison with modified Edlén's formula”, Metrologia 35, 133-139 (1998)

[8] P. E. Ciddor, “Refractive index of air: new equations for the visible and near infrared”, Appl. Opt. 35, 1566-1573 (1996)

[9] A. Lassila and V. Korpelainen, “Acoustic method for determination of the effective temperature and refractive index of air in accurate length interferometry”, Proc. SPIE 4190, 316 (2003)

[10] M. P. Arroyo and R. K. Hansen, “Absorption measurements of water-vapor concentration, temperature, and line-shape parameters using a tunable InGaAsP diode laser”, Appl. Opt. 31, 6104-6116 (1993)

[11] H. Teichert, T. Fernholz, and V. Ebert, “Simultaneous In Situ Measurement of CO, H_2O, and Gas Temperatures in a Full-Sized Coal-Fired Power Plant by Near-Infrared Diode Lasers”, Appl. Opt. 42, 2043-2051 (2003)

[12] T. Hieta and M. Merimaa, “Spectroscopic Measurement of Air Temperature”, Int. J. Thermophysics 31, 1710-1718 (2010)

[13] K. B. Earnshaw and J. C. Owens, “Dual wavelength optical distance measuring instrument, which corrects for air density”, IEEE J. Quantum Electron. 3, 544-550 (1967)

[14] A. Ishida, “Two-Wavelength Displacement-Measuring Interferometer Using Second-Harmonic Light to Eliminate Air-Turbulence-Induced Errors”, Jap. J. of Appl. Phys. 28, L473-L475 (1989)

[15] H. Matsumoto and T. Honda, “High-accuracy length-measuring interferometer using the two-colour method of compensating for the refractive index of air”, Meas. Sci. Technol. 3**,** 1084-1086 (1992)

[16] K. Meiners-Hagen, O. Terra, and A. Abou-Zeid, „Two color interferometry“, Sensoren und Messsysteme 2006: Vorträge der 13. ITG/GMA-Fachtagung vom 13. bis 14.3.2006 in Freiburg/Breisgau (2006)

[17] M. G. Allen, K. L. Carleton et al., “Ultrasensitive dual-beam absorption and gain spectroscopy: applications for near-infrared and visible diode laser sensors”, Appl. Opt. 34, 3240-3249 (1995)

[18] J. A. Silver and D. C. Hovde, “A Comparison of Near-Infrared Diode Laser Techniques for Airborne Hygrometry”, J. Atmos. Oceanic Technol. 15**,** 29 -35 (1998)

[19] B. Schirmer, H. Venzke et al., “High precision trace humidity measurements with a fibre-coupled diode laser absorption spectrometer at atmospheric pressure”, Meas. Sci. Technol. 11, 382-391 (2000)

[20] W. Gurlit, R. Zimmermann el al., “Lightweight diode laser spectrometer CHILD (Compact High-altitude In-situ Laser Diode) for balloonborne measurements of water vapor”, Appl. Opt. 44, 91 – 102 (2005)

[21] G. Durry, N. Amarouche, L. Joly, X. Liu, B. Parvitte and V. Zéninari, “Laser diode spectroscopy of H_2O at 2.63 µm for atmospheric applications, Appl. Phys. B 90, 573 -580 (2008)

[22] Meiners-Hagen K and Abou-Zeid A 2011 A Multiwavelength Interferometer for Geodetic Lengths *accepted for IMEKO 2011*

[23] F. Pollinger, T. Hieta et al., “Effective humidity in length measurements: comparison of three approaches”, submitted to Meas. Sci. Technol.

[24] L. S. Rothman, C. P. Rinsland et al., “The HITRAN molecular spectroscopic database and HAWKS (HITRAN atmospheric workstation): 1996 edition”, J. Quant. Spectrosc. Ra. Trans. 60, 665 – 710 (1998)

[25] L. S. Rothman, I. Gordon et al., “The HITRAN 2008 molecular spectroscopic database”, J. Quant. Spectrosc. Ra. Trans. 110, 533 – 572 (2009)

[26] B. Hardy, “ITS-90 formulations for vapor pressure, frostpoint temperature, dewpoint temperature, and enhancement factors in the range -100 To 100 C”, Proc. 3rd Intern. Symp. on Humidity and Moisture (1998)